



1 *Type of article*

2 **Modeling the transmission dynamics and the impact of the control**
3 **interventions for the COVID-19 epidemic outbreak**

4 **Fernando Saldaña^{1*}, Hugo Flores-Arguedas¹, José Ariel Camacho-Gutiérrez² and Ignacio**
5 **Barradas¹.**

6 ¹ Centro de Investigación en Matemáticas, 36023 Guanajuato, Guanajuato, Mexico

7 ² Facultad de Ciencias, Universidad Autónoma de Baja California, 22860 Baja California, Mexico

8 * **Correspondence:** fernando.saldana@cimat.mx

Abstract: In this paper we develop a compartmental epidemic model to study the transmission dy-
namics of the COVID-19 epidemic outbreak, with Mexico as a practical example. In particular, we
evaluate the theoretical impact of plausible control interventions such as home quarantine, social dis-
tancing, cautious behavior and other self-imposed measures. We also investigate the impact of environ-
mental cleaning and disinfection, and government-imposed isolation of infected individuals. We use a
Bayesian approach and officially published data to estimate some of the model parameters, including
the basic reproduction numbers. Our findings suggest that social distancing and quarantine are the
winning strategies to reduce the impact of the outbreak. Environmental cleaning can also be relevant,
but its cost and effort required to bring the maximum of the outbreak under control indicate that its
cost-efficacy is low.

10 **Keywords:** COVID-19, Epidemic model, Basic reproduction number, Control strategies,
11 **Parameter estimation**

13 **1. Introduction**

14 In late December 2019, the World Health Organization (WHO) received notification of up to 27
15 possible cases of pneumonia of unknown etiology, including 7 severe cases, in the Chinese city of
16 Wuhan. Within a few days, the novel coronavirus, SARS-CoV-2, provisionally named 2019-nCoV,
17 was identified as the causative agent. Since the first report in Wuhan, China, many countries have now
18 reported cases of infection, affecting people of all ages from different origins. Most people with coro-
19 navirus disease (COVID-19), will experience mild to moderate respiratory illness and recover without
20 requiring special treatment. The most common symptoms at the onset of COVID-19 illness are fever,
21 cough, and fatigue, while other symptoms include sputum production, headache, diarrhea, dyspnoea,

1 and lymphopenia, see [13] and the references therein. Older people and those with underlying medical
2 problems are more likely to develop serious illness.

3 On January 30, 2020, the WHO declared COVID-19 as an international emergency and on March
4 11, 2020, the WHO declared the global COVID-19 outbreak a pandemic, pointing to the over 118,000
5 cases of the coronavirus illness in over 110 countries around the world and the constant risk of further
6 spread [12]. The COVID-19 pandemic was confirmed to have reached Mexico in February 2020. On
7 February 28, Mexico confirmed its first three cases. According to the WHO, Mexico entered Phase 2 of
8 the coronavirus pandemic on March 23, 2020, with 367 confirmed cases. Phase 2 includes cases where
9 the sick individuals did not have direct contact with someone who had recently been in another country.
10 As of April 18, there had been 7,497 confirmed cases of COVID-19 in Mexico and 650 reported deaths.

11 According to the Center for Disease Control (CDC), the main transmission route for COVID-19
12 is from person-to-person, either among people in close proximity or through respiratory droplets pro-
13 duced when an infected person coughs or sneezes. Although it is not precisely known the importance
14 of infections caused by contact with contaminated surfaces, the environment-to-person transmission
15 route is also possible, so a person can get COVID-19 by touching a surface or object that has the virus
16 on it and then touching their mouth, nose or eyes. Extensive measures to reduce both person-to-person
17 and environment-to-person transmission of COVID-19 are essential to control the current outbreak.
18 Several countries, including China and the US, have implemented major control interventions, includ-
19 ing travel bans and airport screening. However, the impact of such interventions is probably minor
20 on COVID-19 containment given the potentially large number of asymptomatic individuals and the
21 possibility of transmission before the onset of symptoms [16].

22 Analysis of epidemiological changes in COVID-19 infection is of paramount importance to boost
23 awareness and public health efforts to control the COVID-19 outbreak. In recent years, mathemati-
24 cal modeling has become a valuable tool for the analysis of dynamics of infectious disease and for
25 the support of control strategies development [2]. Mathematical and statistical models are especially
26 useful to estimate key epidemiological parameters such as the basic reproduction number, \mathcal{R}_0 , which
27 is an indicator of the potential severity of an epidemic and provides a powerful tool to estimate the
28 control effort needed to eradicate the disease. Several models, most of them using extensions of
29 the Susceptible-Exposed-Infected-Recovered (*SEIR*) structure, have been proposed to investigate the
30 spread of COVID-19 in different regions [7, 10, 15, 16, 18]. In [9], the authors review current estimates
31 for the basic reproduction number of COVID-19 from 1 January 2020 to 7 February 2020. They found
32 that the estimates range from 1.4 to 6.49, with a mean of 3.28, a median of 2.79 and an interquartile
33 range of 1.16.

34 In this study, we use a mathematical model to investigate the dynamics of the on-going epidemic
35 outbreak of COVID-19. The rest of the paper is structured as follows. In the next section, we for-
36 mulate our model and develop the analysis to compute the basic reproduction number. In Section 3,
37 we calibrate our model using a Bayesian approach and officially published data by the Secretariat of
38 Health, Mexico, corresponding to the daily cumulative cases of infected individuals. In Section 4, we
39 use extensive numerical simulations to investigate the theoretical impact of several control interven-
40 tions against the spread of COVID-19 and compute the effective reproduction number. The last section
41 contains a discussion of the obtained results.

2. Model Formulation Without Control

Based on the clinical progression of the disease, we propose a deterministic compartmental epidemic model under the *SEIR* structure. One important aspect in our model is that, in addition to human-to-human transmission, we consider the indirect infections caused by contact with a contaminated environment.

For our model formulation, we divide the total human population (denoted N) into five compartments: susceptible individuals (denoted S), exposed/latent individuals (denoted E), infectious asymptomatic individuals (denoted A), infectious with symptoms (denoted I), and recovered (denoted R). Finally, we consider a compartment for the free-living COVID-19 in the environment (denoted V).

For our model formulation, we consider a short time horizon in which the total human population is relatively fixed. Therefore, demographic dynamics are not considered in the model. The susceptible population S can acquire the infection when they come in contact with asymptomatic A and symptomatic I infectious individuals at rates β_A and β_I , respectively. They also can be infected by contact with contaminated surfaces with coronavirus at a rate β_V . A proportion p of the exposed individuals E will transition to the symptomatic infectious class I at a rate σ , while the other proportion $1 - p$ will enter the asymptomatic infectious class A . The recovery rates for individuals in the classes A , I are γ_A , γ_I , respectively. These individuals gain permanent immunity and move to the recovered class R . However, individuals in the symptomatic infectious class I can die due to the disease at a rate μ . Asymptomatic and symptomatic infected individuals release virus into the environment with shedding rates c_1 and c_2 , respectively. Hence, the free-living virus in the environment grows with a factor $c_1A + c_2I$. The parameter μ_V represents the mortality rate of the free-living virus in the environment.

These assumptions lead to the following system of differential equations:

$$\begin{aligned}
 \dot{S} &= -\lambda S, \\
 \dot{E} &= \lambda S - \sigma E, \\
 \dot{A} &= (1 - p)\sigma E - \gamma_A A, \\
 \dot{I} &= p\sigma E - \gamma_I I - \mu I, \\
 \dot{R} &= \gamma_A A + \gamma_I I, \\
 \dot{V} &= c_1 A + c_2 I - \mu_V V,
 \end{aligned} \tag{2.1}$$

where $\lambda = \beta_A A + \beta_I I + \beta_V V$ is the force of the infection.

We remark that for the starting model (2.1), we are not including the current intervention measures against coronavirus. This will allow us to focus first on the predictions of the model without control. In Section 4, we incorporate control interventions into our model and investigate the extent of the influence of the controls to prevent coronavirus spread comparing with the case without control.

2.1. Disease-free equilibrium and the basic reproduction number \mathcal{R}_0

The biologically feasible region for model (2.1) is

$$\Omega = \{S, E, A, I, R, V \geq 0 : S + E + A + I + R = N\}. \tag{2.2}$$

Let $X(t)$ be the solution of system (2.1) for a well-defined initial condition $X(0) \in \Omega$. Since $X_i = 0$, implies $\dot{X}_i \geq 0$ for any state variable, then $X(t) \in \Omega$ for all $t > 0$. Thus, solutions trajectories

1 satisfy the usual positiveness and continuity properties and the model is both epidemiologically and
2 mathematically well posed [6].

3 To compute the coordinates of the disease-free equilibrium, we set the rate of change of all state
4 variables equal to zero. Solving the system of algebraic equations we find a unique disease-free equi-
5 librium with the following coordinates:

$$X_o = (S_0, E_0, A_0, I_0, R_0, V_0) = (N_0, 0, 0, 0, 0, 0), \quad (2.3)$$

6 where N_0 is the value of the total population at equilibrium.

7 To compute the basic reproduction number \mathcal{R}_0 , we use the next-generation operator introduced by
8 Diekmann et al. [4]. Under this approach, it is necessary to study the subsystem that describes the
9 production of new infections and changes among infected individuals. The Jacobian matrix \mathbf{J} of this
10 subsystem at the disease-free equilibrium is decomposed as $\mathbf{J} = \mathbf{F} - \mathbf{V}$, where \mathbf{F} is the transmission part
11 and \mathbf{V} describe changes in the infection status. The next-generation matrix is defined as $\mathbf{K} = \mathbf{FV}^{-1}$,
12 and $\mathcal{R}_0 = \rho(\mathbf{K})$, where $\rho(\cdot)$ denotes spectral radius.

For system (2.1), we obtain

$$\mathbf{F} = \begin{bmatrix} 0 & \beta_A S_0 & \beta_I S_0 & \beta_V S_0 \\ 0 & 0 & 0 & 0 \\ 0 & 0 & 0 & 0 \\ 0 & 0 & 0 & 0 \end{bmatrix} \quad \text{and} \quad \mathbf{V} = \begin{bmatrix} \sigma & 0 & 0 & 0 \\ -(1-p)\sigma & \gamma_A & 0 & 0 \\ -p\sigma & 0 & \gamma_I + \mu & 0 \\ 0 & -c_1 & -c_2 & \mu_V \end{bmatrix}.$$

13 Therefore, the basic reproduction number is given by

$$\mathcal{R}_0 = \left[\left(\frac{\beta_A}{\gamma_A} + \frac{c_1 \beta_V}{\mu_V \gamma_A} \right) (1-p) + \left(\frac{\beta_I}{\gamma_I + \mu} + \frac{c_2 \beta_V}{\mu_V (\mu + \gamma_I)} \right) p \right] S_0. \quad (2.4)$$

14 To interpret the biological meaning of the basic reproduction number (2.4), we need the following
15 components. During his infection period, $1/\gamma_A$, an asymptomatic infectious individual produces on
16 average $\beta_A S_0$ infections and c_1 virus particles into the environment. Since the coronavirus survives in
17 the environment a mean time of $1/\mu_V$, the average number of infections caused by the virus is β_V/μ_V .
18 Hence,

$$T_A = \left(\beta_A + c_1 \frac{\beta_V}{\mu_V} \right) \frac{S^0}{\gamma_A} \quad (2.5)$$

19 measure the contribution of asymptomatic infectious individuals to the production of new infections
20 taking into account the environment-to-human transmission route for virus released by asymptomatic
21 individuals. Analogously,

$$T_I = \left(\beta_I + c_2 \frac{\beta_V}{\mu_V} \right) \frac{S^0}{\gamma_I + \mu} \quad (2.6)$$

22 is the contribution of symptomatic infectious individuals to the production of new infections. There-
23 fore, the basic reproduction number (2.4) is the weighted sum of the terms T_A and T_I , that is,

$$\mathcal{R}_0 = (1-p)T_A + pT_I \quad (2.7)$$

24 As a consequence of Theorem 2 in [17], we establish the following result regarding the local stability
25 of the disease-free equilibrium.

1 **Corollary 2.1.** *The disease-free equilibrium of system (2.1) is locally asymptotically stable for $\mathcal{R}_0 < 1$*
 2 *and unstable for $\mathcal{R}_0 > 1$.*

3 In this study, we are interested in the early dynamics of the infection process. Therefore, we did not
 4 consider demographic dynamics and the study of the asymptotic behavior for endemic equilibria.

5 3. Parameter Estimates

6 The compartmental epidemic model (2.1) for the transmission dynamics of SARS-CoV-2 has 11
 7 parameters. First, we gather some parameter values from the literature. Next, we estimate those
 8 parameters that are not found in the literature or that depend on the population under study. We assume
 9 the time unit is days and estimate the parameters as follows.

- 10 (i) *Recovery rates.* The estimated mean value for the recovery rates γ_A, γ_I , for asymptomatic and
 11 symptomatic infectious individuals, respectively, have been estimated to be $\gamma_A = 0.13978$ and
 12 $\gamma_I = 0.33029$ [15].
- 13 (ii) *Mean incubation period.* The mean incubation period ($1/\sigma$) for coronavirus infection has been
 14 estimated to be 6.4 days, ranging from 2.1 to 11.1 days [1]. Therefore, we assume $\sigma = 1/6.4$.
- 15 (iii) *Fraction of individuals which develop symptoms.* The probability of having symptoms after the
 16 infection has been estimated to be $p = 0.868343$ [15].
- 17 (iv) *Mortality rate of coronavirus in the environment.* Some studies have estimated that coronaviruses
 18 can remain infectious on inanimate surfaces at room temperature from a few hours up to 9 days
 19 [8]. Here, we assume an average survival rate of 1 day which implies $\mu_V = 1$.
- 20 (v) *Disease induced death rate.* The estimated mean value for the disease induced death rate is
 21 $\mu = 1.7826 \times 10^{-5}$ [15].

22 The rest of the parameters, that is, the transmission rates β_A, β_I , and β_V , in addition to the shedding
 23 rates c_1 and c_2 , will be estimated using Bayesian inference. We focus on this set of parameters for the
 24 estimation because transmission parameters depend highly on population-level characteristics and it
 25 can be unreliable to take estimations from different data.

26 We consider data corresponding to the daily cumulative cases of infected individuals in Mexico.
 27 The data were obtained from the daily report of the Mexican Secretariat of Health from March 11,
 28 2020, to March 25, 2020 [11]. It is important to remark that this data corresponds to the confirmed
 29 cases; therefore, it is highly possible that the real epidemic curve is higher than the total infected cases
 30 presented in the data. As an attempt to avoid estimates biased down, we fit the data using only the
 31 individuals in the symptomatic infectious class, I , without considering the asymptomatic infectious
 32 class A .

33 The following values were taken as initial conditions: the initial total population was taken as the
 34 approximate Mexican population at the year 2020, i.e., $N(0) = 128,000,000$; the initially symptomatic
 35 infectious individuals as $I(0) = 4$, which is equal to the initial number of confirmed cases in the
 36 data. No recovered individuals are considered at the initial time, thus $R(0) = 0$. Finally, we assumed
 37 $E(0) = 4, A(0) = 1, V(0) = 10$, and $S(0) = N(0) - E(0) - A(0) - I(0)$.

38 For the parameter inference, we use a Bayesian approach. We run a Markov Chain Monte Carlo
 39 (MCMC) using twalk, introduced in [3] (see Appendix A for details). We consider the time in days and
 40 $t_0 = 0$ for the first data on March 11. The resulting total infected cases for the maximum a posteriori

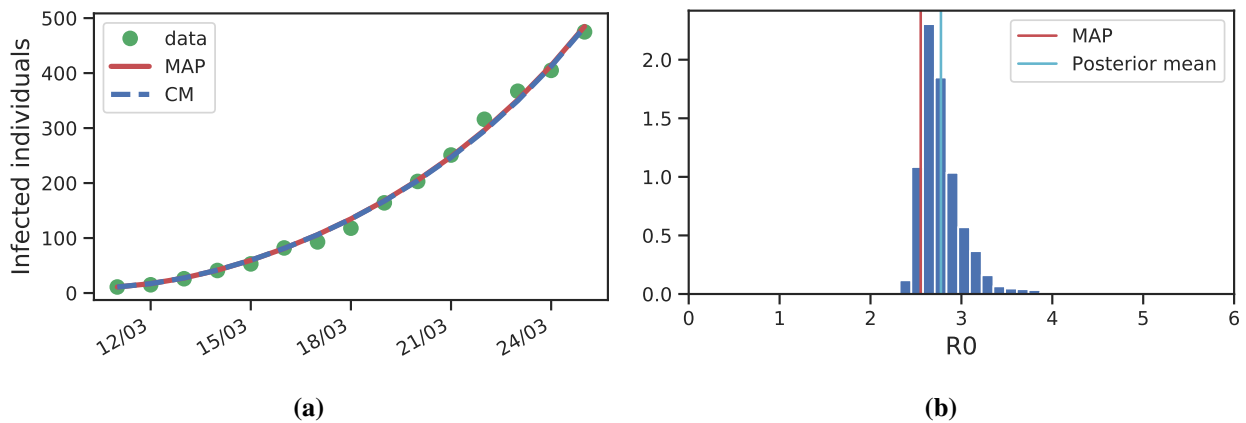


Figure 1. (a) Data per date and fitted curved for the total number of infected individuals in the class $I(t)$ for the MAP estimate and posterior mean. (b) Estimation of \mathcal{R}_0 for the samples of the MCMC. The value of \mathcal{R}_0 for the MAP estimate is 2.5 and for the posterior mean estimate is 2.7.

1 (MAP) and the posterior mean estimates are shown in Fig. 1 (a). The corresponding values for the
 2 parameter estimates are presented in Table 1. In Fig. 1 (b), we show the values for \mathcal{R}_0 corresponding to
 3 the parameter estimates and the elements of the chain. In particular, the value of the basic reproduction
 4 number for the MAP estimate is $\mathcal{R}_0^{MAP} = 2.5$, and for the posterior mean estimate is $\mathcal{R}_0^{CM} = 2.7$; hence,
 5 $\mathcal{R}_0^{MAP} < \mathcal{R}_0^{CM}$. These values are in the range of the current \mathcal{R}_0 estimates [9]. Moreover, please observe
 6 the heavy tail to the right of these values; this heavy tail implies that there exist possible scenarios with
 7 higher \mathcal{R}_0 values (see Fig. 2). (b) for the uncertainty region on the fitted data. Finally, in Fig. 2 (a)
 8 we present the curves of the symptomatic infected class corresponding to the MAP and posterior mean
 9 estimates, $I(t)$, for a time horizon of 200 days.

Parameter	MAP estimate	Posterior mean
β_A	1.32×10^{-14}	1.90×10^{-9}
β_I	6.69×10^{-9}	4.52×10^{-9}
β_V	4.73×10^{-8}	4.88×10^{-8}
c_1	1.89×10^{-6}	2.54×10^{-2}
c_2	1.88×10^{-2}	5.31×10^{-2}

Table 1. Bayesian estimators

10 The posterior distribution obtained allow us to compute posterior predictive marginals for future
 11 data (after March 25). The probability of a future observation \mathbf{z} given the data y is $p(\mathbf{z}|y)$ and can be
 12 computed as follows

$$p(\mathbf{z}|y) = \int_{\mathbb{X}} p(\mathbf{z}|\mathbf{x})p(\mathbf{x}|y)d\mathbf{x} \quad (3.1)$$

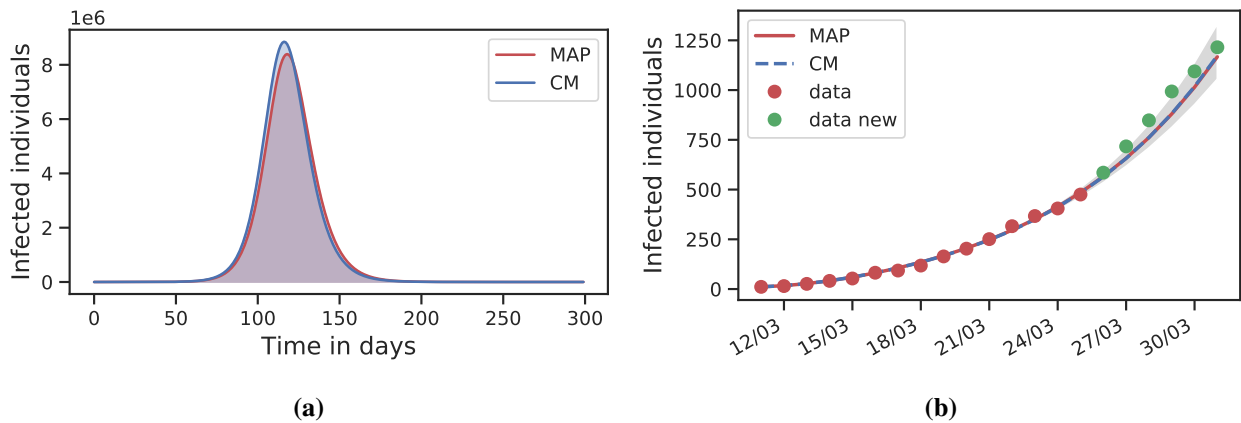


Figure 2. (a) Infectious symptomatic individuals $I(t)$ corresponding to the MAP (red) and the posterior mean estimates (blue). (b) Red dots show the data of cumulative confirmed cases of COVID-19 in Mexico from March 11, 2020, to March 25, 2020. The gray area shows the uncertainty with the last 25000 samples of the chain. The green dots represent data from March 26 to March 31 that were not used in the inference.

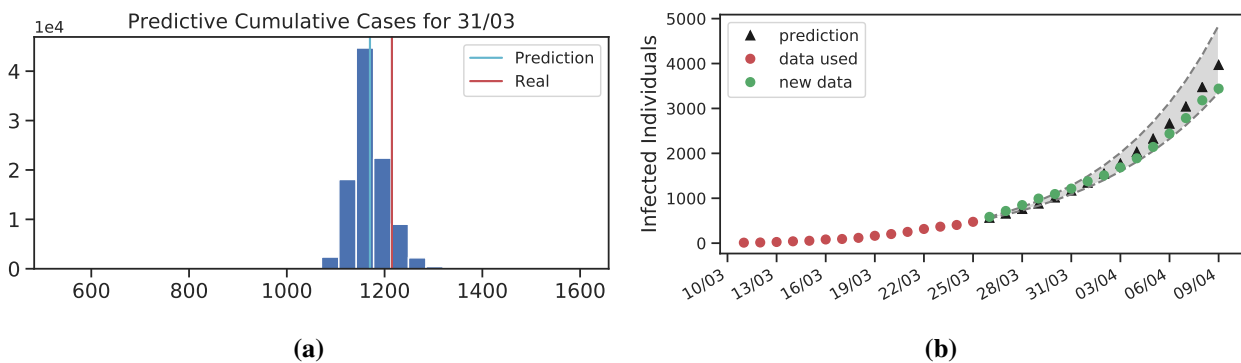


Figure 3. (a) Posterior predictive marginal for the total cumulative infections on March 31. (b) Red dots show the data of cumulative confirmed cases of COVID-19 in Mexico from March 11, 2020, to March 25, 2020, used for the inference. In black we present our predicted values, in green the data from March 26 to April 9 not used in the inference, and the dashed lines show the interval with 98 percent of the mass for the predictive marginal.

1 where \mathbf{x} denotes our vector of parameters. Figure 3 (a) shows the predictive posterior marginal for
 2 the total cumulative infections on March 31. Figure 3 (b) shows a comparison between the predicted
 3 values for the cumulative number of infections and the officially published data from March 26 to April
 4 9. The dashed lines represent the interval with 98 percent of the mass for the predictive marginal.

5 According to our estimations, the value of the basic reproduction number \mathcal{R}_0 in the absence of
 6 control is above unity. Under a non-intervention scenario, we expect that the number of individuals
 7 in the infectious class $I(t)$ to have a high peak that can produce a collapse in the health care system.
 8 Therefore, it is of paramount importance the application of effective control measures to limit the
 9 spread of SARS-CoV-2 and flatten the epidemic curve.

4. Control Interventions

In this section, we extend the compartmental epidemic model for COVID-19 transmission dynamics (2.1) including appropriate compartments to take into account some of the current intervention measures for COVID-19 control. In particular, we consider the following control interventions:

- (i) Social distancing and home quarantine.
- (ii) Isolation of infected individuals.
- (iii) Environmental cleaning and disinfection.

For modeling social distancing and home quarantine in our model, we assume susceptible individuals S change their behavior and become cautious susceptible individuals (denoted S_c) at a rate α . The parameter α is the rate of behavioral change. This may be increased through mass communication (TV, social networks, etc.). Cautious susceptible individuals will reduce their probability of infection by a factor $1 - \theta \in (0, 1)$ taking appropriate measures such as self-imposed home quarantine, social distancing, hand washing, and mask-wearing. To model isolation, we assume that symptomatic infected individuals, I , are screened at a rate d_2 and moved to a diagnosed compartment D . Likewise, individuals in the exposed and asymptomatic classes are diagnosed at a rate d_1 . It should be easier to identify infected people with strong symptoms in comparison to asymptomatic individuals, therefore, $d_2 > d_1 \geq 0$. We assume individuals in the D class are being isolated and treated. Finally, we consider cleaning of visibly dirty surfaces followed by disinfection which is an important practice measure for the prevention of COVID-19. We model this by considering an additional mortality rate m for the free virus V .

From the above considerations, the control model for the transmission dynamics of COVID-19 is governed by the following equations:

$$\begin{aligned}
 \dot{S} &= -\lambda S - \alpha S, \\
 \dot{S}_c &= -\lambda\theta S_c + \alpha S, \\
 \dot{E} &= \lambda(S + \theta S_c) - \sigma E - d_1 E, \\
 \dot{A} &= (1 - p)\sigma E - d_1 A - \gamma_A A, \\
 \dot{I} &= p\sigma E - d_2 I - \gamma_I I - \mu I, \\
 \dot{D} &= d_1(E + A) + d_2 I - \gamma_D D - \mu D, \\
 \dot{R} &= \gamma_A A + \gamma_I I + \gamma_D D, \\
 \dot{V} &= c_1 A + c_2 I - (\mu_V + m)V,
 \end{aligned} \tag{4.1}$$

where $\lambda = \beta_A A + \beta_I I + \beta_V V$ is the force of the infection.

The disease-free equilibrium for system (4.1) is of the form

$$\tilde{X}_o = (0, N_0, 0, 0, 0, 0, 0, 0). \tag{4.2}$$

Defining the vector of constant controls $u = (\alpha, 1 - \theta, d_1, d_2, m)$ and using the next-generation matrix, we obtain the following expression for the effective reproduction number \mathcal{R}_e :

$$\mathcal{R}_e(u) = (1 - p)\tilde{T}_A(u) + p\tilde{T}_I(u) \tag{4.3}$$

1 where

$$\tilde{T}_A(u) = \frac{\sigma}{(d_1 + \gamma_A)(\sigma + d_1)} \left(\beta_A + \frac{c_1 \beta_V}{\mu_V + m} \right) \theta N_0 \quad (4.4)$$

2 is the contribution of asymptomatic infectious individuals A to the production of new infections, and

$$\tilde{T}_I(u) = \frac{\sigma}{(d_2 + \gamma_I + \mu)(\sigma + d_1)} \left(\beta_I + \frac{c_2 \beta_V}{\mu_V + m} \right) \theta N_0 \quad (4.5)$$

3 is the contribution of the symptomatic infectious individuals I to the incidence. Please note that $\tilde{T}_j(0) =$
 4 T_j ($j = \{A, I\}$), therefore, in the absence of controls, the effective reproduction number is equal to the
 5 basic reproduction number, $\mathcal{R}_e(0) = \mathcal{R}_0$.

6 4.1. The impact of social distancing and home quarantine

7 Here, we investigate the impact of cautious behavior of susceptible individuals, which results in
 8 self-imposed prevention measures such as social distancing and home quarantine. In mathematical
 9 terms, we explore how our model dynamics depends on the control parameters α and θ . The rest of the
 10 control parameters are not considered here.

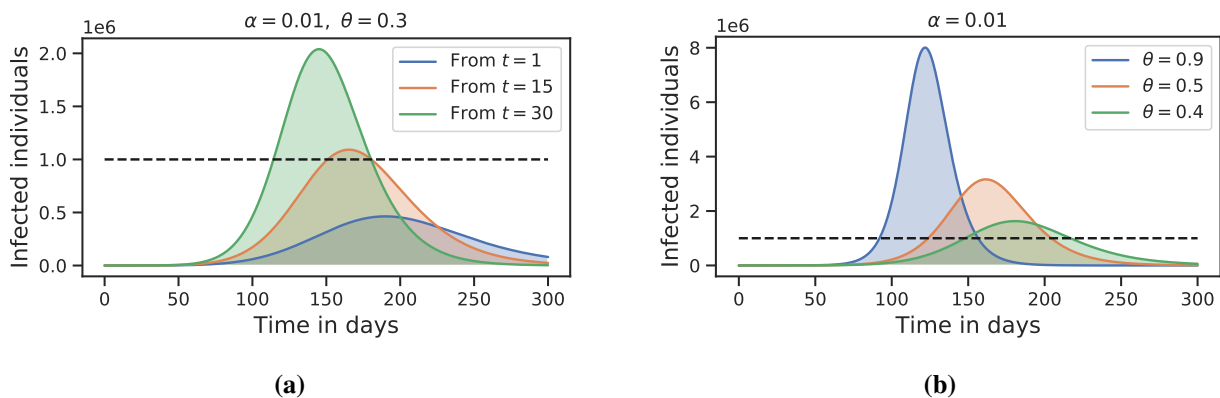


Figure 4. Dynamics of the symptomatic infected class, $I(t)$, under the control measure which represents cautious behavior of susceptible individuals. Dashed lines represent hypothetical health-care system capacity. **(a)** We investigate three possible initial times for the application of the control intervention: $t = 1$ (blue), $t = 15$ (orange), and $t = 30$ (green) with $\alpha = 0.01$, and $\theta = 0.3$. **(b)** We explore different values for the control parameter θ , for all values the initial application time is $t = 1$ and $\alpha = 0.01$.

11 We assume susceptible individuals in the susceptible cautious class reduce their probability of in-
 12 fection by a factor $1 - \theta$ for different values of the parameter θ , and we set the rate of behavioral change
 13 as $\alpha = 0.01$. It should be pointed out that the values of these parameters used in the simulations are
 14 theoretical as they were chosen with the purpose of highlight the possible impact of the control mea-
 15 sures proposed in this study. This will allow us to focus on the investigation of the role played by the
 16 initial times for the application of the intervention to flatten the prevalence curve. In particular, we
 17 explore three possible initial times for the application of the intervention: (i) since day one ($t = 1$),
 18 (ii) since two weeks after the first confirmed cases ($t = 15$), and (iii) since a month after the first cases
 19 ($t = 30$). For the sake of simplicity, we assume that after the initial time of application the intervention

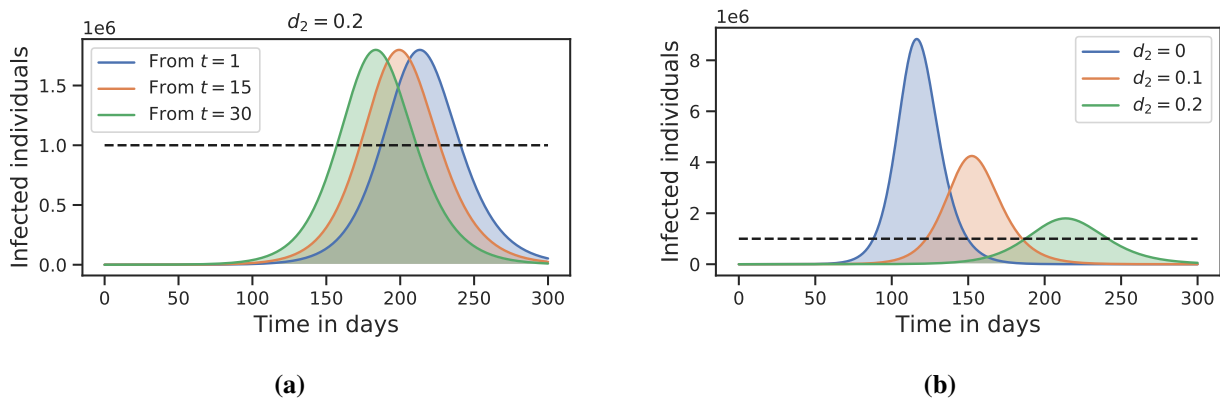


Figure 5. Dynamics of the symptomatic infected class, $I(t)$, under the control measure which represents isolation of infected individuals. Dashed lines represent hypothetical health-care system capacity. **(a)** We investigate three possible initial times for the application of the control intervention: $t = 1$ (blue), $t = 15$ (orange), and $t = 30$ (green) with $d_2 = 0.02$, and $d_1 = 2.0$. **(b)** We explore different values for the control parameters d_1 and d_2 with $10d_1 = d_2$, for all values the initial application time is $t = 1$.

1 is maintained for the whole time horizon. Since some of the posterior distributions have heavy tails
 2 (see Appendix A), for all the subsequent numerical simulations, the non-control parameters are fixed
 3 using the posterior mean estimates.

4 The results are shown in Figure 4. Dashed lines represent hypothetical health-care system capacity.
 5 Please observe that social distancing and home quarantine as control measures have the potential to
 6 reduce the maximum number of infected individuals at the peak of the outbreak and also delay the
 7 time of peak. Hence, this intervention has the potential to flatten the epidemic curve. From Figure 4
 8 (a), one can also notice that a delayed introduction of control measures increases a lot the size of the
 9 peak. For our parameters, a fifteen days delay in the use of the control causes, roughly, the number of
 10 cases at the peak to double. From Figure 4 (b), it can be observed that small variations in the parameter
 11 θ have a big effect on the epidemic curve. Hence, increasing the effectiveness of social distancing and
 12 home quarantine will produce a huge benefit to reduce the prevalence of the infection.

13 4.2. The impact of isolation of infected individuals

14 In this section, we analyze the effect of isolation of infected individuals. Therefore, we focus on the
 15 screening/diagnosed rates d_1 and d_2 . In Mexico, according to some early reports, only 10 percent of
 16 mild suspected cases are tested for COVID-19 [5]. On the other hand, for severe cases, 100 percent of
 17 patients are tested. Hence, we assume $10d_1 = d_2$. In particular, we take $d_2 = 0.02$, and $d_1 = 2.0$ and
 18 explore how the initial time of control application influence the possible prevalence of the infection.
 19 For our simulations, the parameters which are already described by the model without control (2.1) are
 20 fixed with their posterior mean estimate. In addition, we take $\gamma_D = 0.1162$ from [15].

21 The results are presented in Figure 5. We can see that the diagnosis and isolation of infected
 22 individuals will reduce the maximum number of infected individuals in comparison with the no control
 23 case (see Figure 2). It is noteworthy to mention (see Figure 5 (a)) that for this intervention, the initial
 24 application of the control does not influence the size of the peak number of diagnoses and only moves

1 the peak's timing. However, the value of the control parameters has the potential to reduce the size of
 2 the peak number of diagnoses and delay its occurrence (Figure 5 (b)).

3 4.3. The impact of environmental cleaning and disinfection

4 It has been documented that SARS-CoV-2 can be deposited onto everyday surfaces in a household
 5 or hospital setting by an infected person through coughing or touching objects and that the virus is
 6 transmissible through relatively casual contact with contaminated surfaces [8]. Hence, we analyze the
 7 effect of environmental cleaning and disinfection as a measure to prevent COVID-19 spread. Hence,
 8 we study the effect of the parameter m related to an increase in the death rate of the virus that remains
 9 in contaminated surfaces.

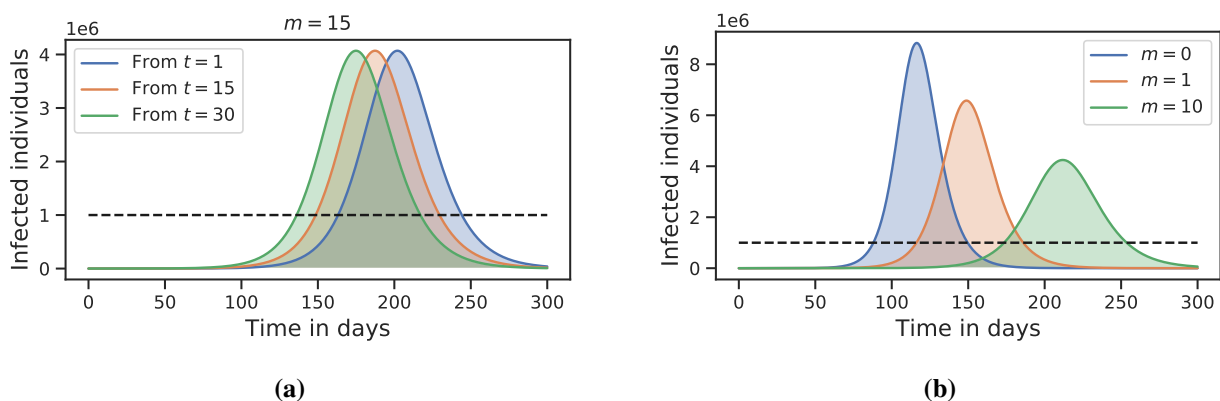


Figure 6. Dynamics of the symptomatic infected class, $I(t)$, under the control measure which represents environmental cleaning and disinfection. Dashed lines represents hypothetical health-care system capacity. **(a)** We investigate three possible initial times for the application of the control intervention: $t = 1$ (blue), $t = 15$ (orange), and $t = 30$ (green) with $m = 15$. **(b)** We explore different values for the control parameter m , for all values the initial application time is $t = 1$.

10 The simulations in Figure 6 show that analogously to the case of the isolation measure, for this
 11 intervention the initial application of the control does not influence the size of peak and only moves the
 12 peak's time (see Figure 6 (a)). An increase in the value of m has the potential to flatten the epidemic
 13 curve, however, big increments in m are needed to reduce substantially the prevalence of the infection
 14 below the theoretical health-care system capacity (see Figure 6 (b)). Therefore, under this strategy
 15 alone will be difficult to successfully prevent further spread of COVID-19.

16 4.4. Combination of control strategies

17 In this section, we investigate the extent of the impact of using our three control interventions
 18 simultaneously. As China and South Korea have demonstrated [14], social distancing is an effective
 19 measure to slow the spread of the virus and limit how many people are infected at one time. However,
 20 there is a lot of uncertainty about how long social distancing will have to last to reduce the spread of
 21 COVID-19 to near zero. Therefore, we focus on exploring the effect of different quarantine's duration
 22 on the reduction of the prevalence.

In particular, in the numerical simulations, three possible social distancing and home quarantine's duration are analyzed: one month, two months and three months. The illustrative simulations of these scenarios are presented in Figure 7 (a). The values of the control parameters during active social distancing are $\alpha = 0.01$, $\theta = 0.4$, $d_1 = 15$, $d_2 = 0.15$, $m = 5$. After the application of home quarantine and social distancing the parameters d_1 , d_2 , m keep the same value but the parameters α and θ are turned off. The simulations (see Figure 7 (a)) show the unexpected result that extending quarantine duration does not reduce the size of the peak number of diagnoses and only moves the peak's timing. Considering the results in Figure 4, one can deduce that the most influencing factor for the efficacy of social distancing, home quarantine, and other lockdown measures is the timing. Hence, these measures must be put in use as soon as possible by health authorities.

Another important scenario that is of interest for public health officials is if there will be a need for several rounds of social distancing and home quarantine. As an illustrative example, we simulate the periodic application of the control interventions for one week, two weeks and a month. That is, for example, the interventions are used for one month, then turned off for the next month and then turned on for the next month periodically. The results are shown in Figure 7 (b). Please observe that this brings oscillations in the prevalence of the infection. The oscillations increase their altitude and amplitude with a larger time frame for the control interventions. In this case, when the control is on, the values for the parameters are $\alpha = 0.01$, $\theta = 0.4$, $d_1 = 20$, $d_2 = 0.2$, $m = 5$.

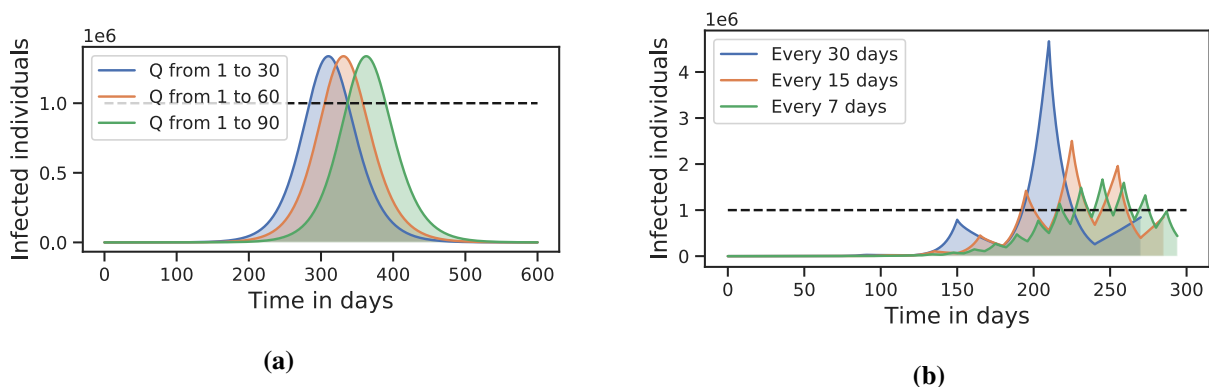


Figure 7. Dynamics of the symptomatic infected class, $I(t)$, under the application of the three control interventions. Dashed lines represent hypothetical health-care system capacity. **(a)** We investigate three possible quarantine's duration: one month (blue), two months (orange), and three months (green). **(b)** We explore how the periodic application of the control interventions affects the epidemic curve.

5. Discussion

In this study, we have proposed a compartmental epidemic model to model the transmission dynamics of the COVID-19 epidemic. Our model formulation is based on the *SEIR* structure augmented with appropriate compartments to take into account the current intervention measures against the spread of SARS-CoV-2. Moreover, in addition to human-to-human transmission, our model considers indirect infections caused by contact with contaminated surfaces using an extra compartment for the free-living coronavirus in the environment. We used a Bayesian approach and officially published data to calibrate

1 the model and estimate the basic reproduction number \mathcal{R}_0 .

2 The results of our Bayesian inference show that the value of the basic reproduction number for
3 the MAP estimate is $\mathcal{R}_0^{MAP} = 2.5$, and for the posterior mean estimate is $\mathcal{R}_0^{CM} = 2.7$. Moreover,
4 under a non-intervention scenario, the model outcome shows that the maximum number of infected
5 individuals at the peak of the outbreak will be very high and can produce a collapse in the health care
6 system. Therefore the importance of prompt implementation of effective interventions to prevent the
7 further spread of COVID-19.

8 After our model calibration, we incorporated some of the current control interventions against
9 COVID-19 into our model: (i) social distancing and home quarantine, (ii) isolation of infected individ-
10 uals, and (iii) environmental cleaning and disinfection. We present illustrative numerical simulations
11 as a tool to evaluate the theoretical impact of our control interventions for plausible scenarios related
12 to the effectiveness and duration of the control application. In particular, we first study the effect of
13 each of our interventions alone and the role played by the initial times of the application of the control
14 to flatten the epidemic curve.

15 The results of our numerical simulations suggest that social distancing and home quarantine as
16 control measures have the potential to reduce the maximum number of infected individuals at the peak
17 of the outbreak and also delay the time of peak. Hence, this intervention alone has the potential to
18 flatten the epidemic curve. However, this intervention should be implemented as soon as possible
19 because a delayed introduction increases a lot the size of the peak of the infected. In particular, a
20 fifteen days delay in the use of this intervention causes, roughly, the number of cases at the peak to
21 double. The simulations also show that the diagnosis and isolation of infected individuals will reduce
22 the size of the peak number of diagnoses and delay its occurrence. However, to successfully control
23 the infection more effort is needed under this intervention in comparison with social distancing and
24 quarantine. The impact of environmental cleaning and disinfection to reduce the prevalence is low,
25 thus, with this strategy alone will be very difficult to achieve disease eradication.

26 Comparing the three strategies presented here, we observe that social distancing and quick isolation
27 of infected individuals are better strategies. Environmental cleaning can also be relevant, but its cost
28 and effort required to bring the maximum of the outbreak under control indicate that it might be too
29 expensive for the results. It is noteworthy to mention that the initial application of the control does not
30 influence the maximum number of infected individuals at the peak of the outbreak for the isolation and
31 environmental cleaning strategies, so the winning strategy, besides being applied as soon as possible,
32 seems to be social distancing and home quarantine. In separate work, we compare the effect of similar
33 percentage changes for each of the three parameters and their relative effect on the outcome of the
34 epidemics. We expect social distancing and quarantine to also be the best strategies.

35 Acknowledgments

36 Fernando Saldaña acknowledge the support by The National Council of Science and Technology,
37 CONACyT, Mexico under grant number 331194. Ariel Camacho acknowledge SEP-PRODEP-UABC
38 for Post-doctoral Fellowship support. Hugo Flores Arguedas acknowledge the support by The National
39 Council of Science and Technology, CONACyT, Mexico under grant number 334204.

1 Conflict of interest

2 The authors declare no conflicts of interest in this paper.

3 References

- 4 1. Backer, J. A., Klinkenberg, D., and Wallinga, J. (2020). Incubation period of 2019 novel coronavirus
5 (2019-ncov) infections among travellers from wuhan, china, 20–28 january 2020. *Eurosurveillance*,
6 25(5).
- 7 2. Brauer, F. (2017). Mathematical epidemiology: Past, present, and future. *Infectious Disease Mod-*
8 *elling*, 2(2):113–127.
- 9 3. Christen, J. A., Fox, C., et al. (2010). A general purpose sampling algorithm for continuous distri-
10 butions (the t-walk). *Bayesian Analysis*, 5(2):263–281.
- 11 4. Diekmann, O., Heesterbeek, J. A. P., and Metz, J. A. (1990). On the definition and the computation
12 of the basic reproduction ratio r_0 in models for infectious diseases in heterogeneous populations.
13 *Journal of mathematical biology*, 28(4):365–382.
- 14 5. El Financiero. Al 10% de los casos sospechosos de covid-19 con síntomas leves se les aplica prueba:
15 Imss.
- 16 6. Hethcote, H. W. (2000). The mathematics of infectious diseases. *SIAM review*, 42(4):599–653.
- 17 7. Jia, J., Ding, J., Liu, S., Liao, G., Li, J., Duan, B., Wang, G., and Zhang, R. (2020). Modeling
18 the control of covid-19: Impact of policy interventions and meteorological factors. *arXiv preprint*
19 *arXiv:2003.02985*.
- 20 8. Kampf, G., Todt, D., Pfaender, S., and Steinmann, E. (2020). Persistence of coronaviruses on
21 inanimate surfaces and its inactivation with biocidal agents. *Journal of Hospital Infection*.
- 22 9. Liu, Y., Gayle, A. A., Wilder-Smith, A., and Rocklöv, J. (2020). The reproductive number of
23 covid-19 is higher compared to sars coronavirus. *Journal of travel medicine*.
- 24 10. Nadim, S. S., Ghosh, I., and Chattopadhyay, J. (2020). Short-term predictions and prevention
25 strategies for covid-2019: A model based study. *arXiv preprint arXiv:2003.08150*.
- 26 11. of Health, S. (2020). Aviso epidemiológico: casos de infección respiratoria asociados a nuevo-
27 coronavirus-2019-ncov. [urlhttps://www.gob.mx/salud/es](https://www.gob.mx/salud/es).
- 28 12. Organization, W. H. et al. (2020). Coronavirus disease 2019 (covid-19): situation report, 51.
- 29 13. Rothan, H. A. and Byrareddy, S. N. (2020). The epidemiology and pathogenesis of coronavirus
30 disease (covid-19) outbreak. *Journal of Autoimmunity*, page 102433.
- 31 14. Shim, E., Tariq, A., Choi, W., Lee, Y., and Chowell, G. (2020). Transmission potential and severity
32 of covid-19 in south korea. *International Journal of Infectious Diseases*.
- 33 15. Tang, B., Wang, X., Li, Q., Bragazzi, N. L., Tang, S., Xiao, Y., and Wu, J. (2020). Estimation of
34 the transmission risk of the 2019-ncov and its implication for public health interventions. *Journal of*
35 *Clinical Medicine*, 9(2):462.

16. Teslya, A., Pham, T. M., Godijk, N. E., Kretzschmar, M. E., Bootsma, M. C., and Rozhnova, G. (2020). Impact of self-imposed prevention measures and short-term government intervention on mitigating and delaying a covid-19 epidemic. *medRxiv*.
17. Van den Driessche, P. and Watmough, J. (2002). Reproduction numbers and sub-threshold endemic equilibria for compartmental models of disease transmission. *Mathematical biosciences*, 180(1-2):29–48.
18. Yang, C. and Wang, J. (2020). A mathematical model for the novel coronavirus epidemic in wuhan, china. *Mathematical Biosciences and Engineering*, 17(3):2708.

A. Bayesian Inference

For the Bayesian inference, we assume the following model for the data y_i

$$y_i = C(t_i; \mathbf{x}) + \eta_i, \quad i = 0, \dots, 14 \quad (\text{A.1})$$

where $C(t_i; \mathbf{x})$ denote the cumulative cases built from the solution I of the ODE's system at time t_i and $\mathbf{x} = (\beta_A, \beta_I, \beta_V, c_1, c_2)$ is the vector of parameters to estimate. We assume independence in the realizations of \mathbf{x} and η and $\eta_i \sim \mathcal{N}(0, \sigma^2)$. Our cumulative infected cases satisfies $C(0; \mathbf{x}) = y_0$ and

$$C(t_i; \mathbf{x}) = C(0; \mathbf{x}) + \sum_{k=0}^{k=i} I(t_k; \mathbf{x}) \quad (\text{A.2})$$

where $I(t_k; \mathbf{x})$ denote the infected cases at time t_k given by the solution for the I class in our model given the parameter \mathbf{x} . Moreover, we define by $\pi_0(\mathbf{x})$ the prior distribution for \mathbf{x} . We assume independence of the parameters, hence

$$\pi_0(\mathbf{x}) = \pi_1(\beta_A)\pi_2(\beta_I)\pi_3(\beta_V)\pi_4(c_1)\pi_5(c_2) \quad (\text{A.3})$$

where we propose gamma distributions for β_A and c_1 and uniforms for the rest. Recall that the gamma distribution is denoted by $\Gamma(\alpha, \beta)$ with α the shape parameter and β the inverse scale parameter. If $Z \sim \Gamma(\alpha, \beta)$ then $\mathbb{E}[Z] = \alpha/\beta$ and $\text{Var}[Z] = \alpha/\beta^2$. We propose

$$\begin{aligned} \beta_A &\sim \Gamma(1, 10^8) \\ \beta_I &\sim U(0, 10^{-1}) \\ \beta_V &\sim U(0, 10^{-1}) \\ c_1 &\sim \Gamma(1, 10^3) \\ c_2 &\sim U(0, 1) \end{aligned} \quad (\text{A.4})$$

where $U(a, b)$ denote the uniform distribution in the interval (a, b) . We run a MCMC using twalk for 2000000 samples with 1000000 of burnin. The posterior distribution for each parameter are shown in Fig. 8.



AIMS Press

©2020 the Author(s), licensee AIMS Press. This is an open access article distributed under the terms of the Creative Commons Attribution License (<http://creativecommons.org/licenses/by/4.0>)

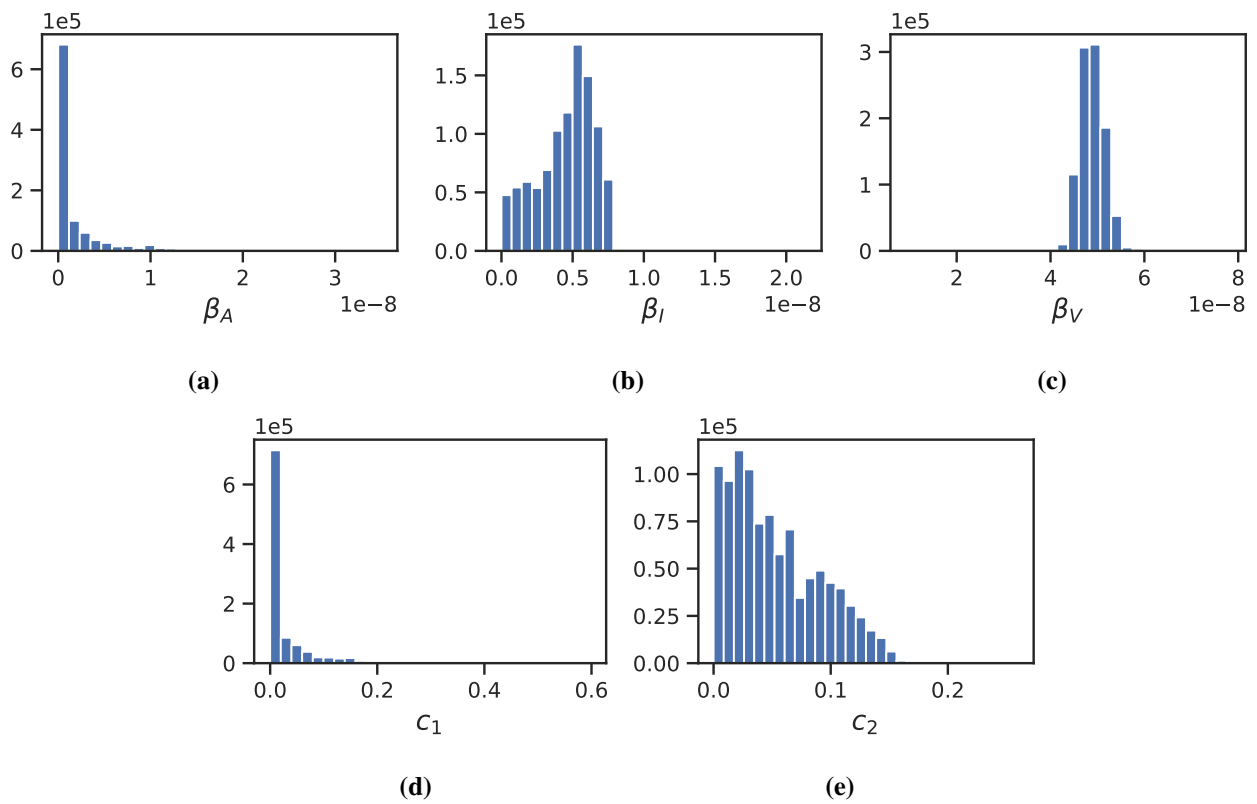


Figure 8. Posterior distributions for the parameters: **(a)** β_A , **(b)** β_I , **(c)** β_V , **(d)** c_1 , **(e)** c_2 . The parameters β_A and c_1 are not well informed by the data, their posterior distribution corresponds to its prior distribution.

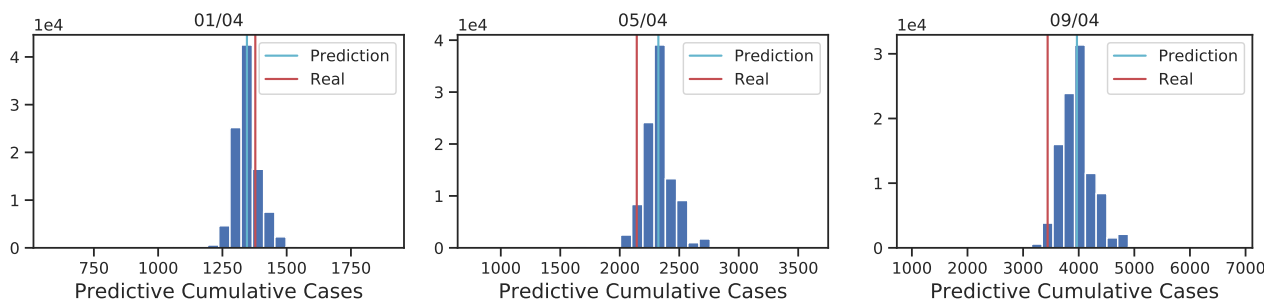


Figure 9. Posterior predictive marginals for the total cumulative infections for several dates